PERGAMON

European Journal of Cancer 39 (2003) 1105–1114

European Journal of Cancer

www.ejconline.com

Population pharmacokinetic modelling of unbound and total plasma concentrations of paclitaxel in cancer patients

A. Henningsson[a,*], A. Sparreboom[b,1], M. Sandström[a], A. Freijs[a], R. Larsson[c], J. Bergh[d], P. Nygren[e], M.O. Karlsson[a]

[a]*Division of Pharmacokinetics and Drug Therapy, Department of Pharmaceutical Biosciences, Faculty of Pharmacy, Uppsala University, Box 591, SE-751 24 Uppsala, Sweden*
[b]*Department of Medical Oncology, Erasmus Mc-Daniel den Hoed Cancer Center, 3075 EA Rotterdam, The Netherlands*
[c]*Department of Medical Sciences, Division of Clinical Pharmacology, University Hospital, SE-751 85 Uppsala, Sweden*
[d]*Department of Oncology, Radiumhemmet, Karolinska Hospital, SE-171 76 Uppsala, Sweden*
[e]*Department of Oncology, Radiology and Clinical Immunology, University Hospital, SE-751 85 Uppsala, Sweden*

Received 8 May 2002; received in revised form 2 December 2002; accepted 24 January 2003

Abstract

The aim of this study was to validate and further develop a mechanism-based population pharmacokinetic model for paclitaxel (Taxol®; Bristol-Myers Squibb Co, Princeton, NJ, USA) based on the knowledge of Cremophor EL (CrEL) micelle entrapment and to evaluate the exposure/toxicity relationships. Paclitaxel (total and unbound) and CrEL concentrations were obtained according to a sparse sampling scheme with on average only 3.5 samples per course from 45 patients with solid tumours who received 3-hour infusions of paclitaxel (final dose range 112–233 mg/m^2). The present data were predicted well by the mechanism-based model. In addition, bilirubin and body size were found to be significant as covariates. A change in body surface area (BSA) of 0.1 m^2 typically caused a change in clearance (CL) of 22.3 l/h and an increase in bilirubin of 10 μM typically caused a decrease in CL of 41 l/h. Toxicity was best described by a threshold model. In conclusion, even with a sparse sampling scheme, the same mechanism-based binding components as in the previously developed model could be identified. Once the CrEL and total paclitaxel plasma concentrations are known, the unbound concentrations, which are more closely related to the haematological toxicity, can be predicted.

Keywords: Paclitaxel; Cremophor EL; Pharmacokinetics; Pharmacodynamics

1. Introduction

The non-linear pharmacokinetics of paclitaxel in plasma has been described in several studies. The non-linearity has mostly been described as both saturable elimination and distribution (saturable transport [1] or saturable binding [2]), but also as caused by the micelle-forming vehicle Cremophor EL (CrEL) [3–5]. CrEL has been suggested to inhibit P-glycoprotein-mediated biliary secretion [6], cause lipoprotein dissociation that would alter protein binding [7] and, recently, it has been suggested to cause an alteration in the distribution in human blood by entrapment in micelles [5]. The free fraction of paclitaxel has been shown to decrease with increasing CrEL concentrations [5]. Paclitaxel has previously been shown to bind to both albumin and α_1-acid glycoprotein [8]. In our previous model [9], the non-linearity could be explained to a large extent by binding that was directly proportional to the CrEL concentration.

The pharmacokinetic/pharmacodynamic (PK/PD) relationship for paclitaxel toxicity has previously been described by a threshold model [6,10] and also by more general models using a non-linear continuous function [11,12]. Since the free fraction of paclitaxel has been shown to vary over time and the drug effect is generally considered to be more closely related to the unbound

* Corresponding author. Tel.: +46-18-471-4385; fax +46-18-471-4003.
E-mail address: anja.henningsson@farmbio.uu.se (A. Henningsson).
[1] Current address: Clinical Pharmacology Research Core, Medical Oncology Clinical Research Unit, National Cancer Institute, Bethesda, MD 20892, USA.

0959-8049/03/$ - see front matter
doi:10.1016/S0959-8049(03)00126-6

drug, the PK/PD relationship based on the total concentration needs to be re-evaluated.

The aim of this study was to validate a previously developed mechanism-based population pharmacokinetic model that describes unbound and total plasma concentrations of paclitaxel, to extend the model with covariates and, based on new toxicity data, to characterise the PK/PD relationship based on unbound and total concentrations of paclitaxel.

2. Patients and methods

This study included 14 male and 31 female patients with different types of solid tumours (colorectal, gastric, gall bladder, breast, uterine, ovarian, pancreas) at advanced stages, not amenable to standard therapy. They received paclitaxel as a 3-hour intravenous (i.v.) infusion with an initial dose of 175 mg/m^2 every third week within a trial on the feasibility of chemotherapy selection based on drug sensitivity testing *ex vivo*. Dose adjustments, escalations and reductions, were based on any associated haematological and non-haematological toxicity, which resulted in a final dose range of 112–233 mg/m^2. Plasma concentrations were monitored on courses 1 and 3 (75 concentration–time profiles in total). Peripheral venous blood samples were collected following a sparse sampling scheme with four nominal sampling times at 1.5, 3 (just before the finish of the infusion), 8 and 21 h. The sparse sampling scheme was a compromise for taking into account the constraints imposed by an out-patient study and also the possibility estimate the maximal concentration (C_{max}) and area under the concentration curve (AUC). It should be noted that at the time of the study design, we did not have the mechanism-based model and did not know that unbound paclitaxel and CrEL should be measured. Unbound and total concentrations of paclitaxel, 243 and 275 observations, respectively, and the actual sampling times (on average 3.5 per course) can be seen in Fig. 1. The discrepancy in the number of observations between unbound and total concentrations was due to the fact that the unbound concentrations were measured after the total and there were not enough matrices left for all of the time points. Plasma samples were stored at −80 °C until analysis.

Blood samples for the assessment of haematological toxicity were collected weekly. The lowest observed value was used as the nadir and the pre-course values were used as the baseline. Baseline and nadir values of absolute neutrophil count (ANC) were obtained on the courses where PK data were available and where information about the neutrophils were available for at least two weeks after the infusion. Three individuals were excluded due to high and increasing values of ANC. In total, 36 individuals (53 courses) were included in the toxicity analysis. Patient characteristics are given in Table 1. The study was approved by the Ethical Committee at Uppsala University Hospital and all patients gave their informed consent according to the Declaration of Helsinki.

2.1. Bioanalysis

Total paclitaxel concentrations were measured with a reversed phase high performance liquid chromatography method with ultraviolet (UV) detection at 227 nm as described earlier in Refs. [11,13]. The limit of

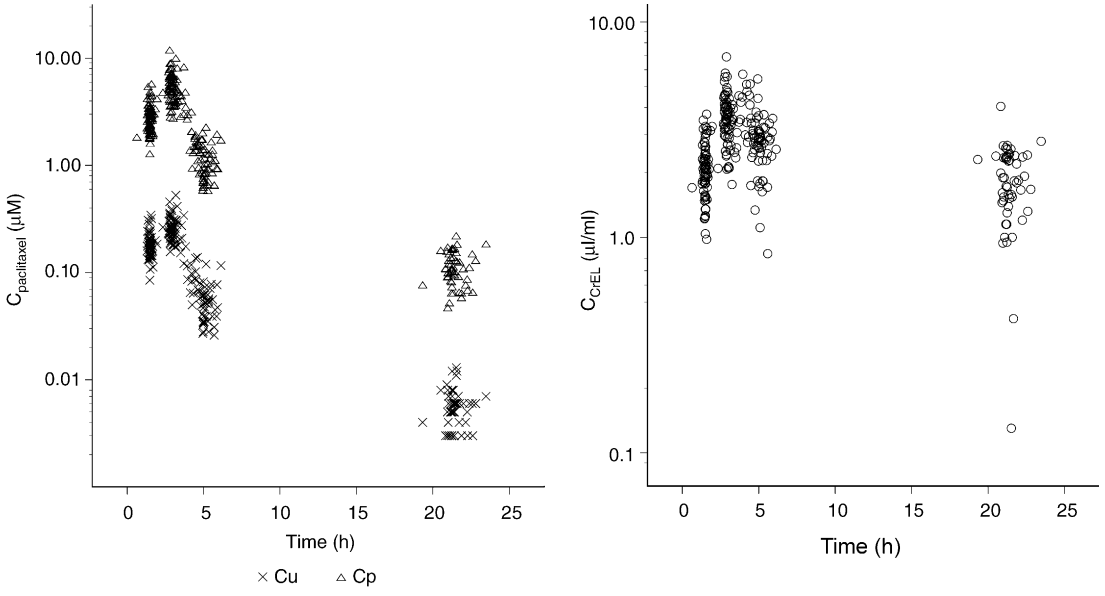

Fig. 1. The left panel shows observed unbound, C_u, and total concentrations, C_p, of paclitaxel versus time and the right panel shows observed concentrations of Cremophor EL (CrEL) versus time.

Table 1
Patient characteristics

Continuous covariates	Number of observations	Median (range)
Age (years)	75	57 (23–71)
Height (cm)	73	169 (149–190)
Weight (kg)	68	68 (34–93)
BSA (m^2)	72	1.76 (1.35–2.15)
CL_{CR} (ml/min)	64	77 (41–166)
Albumin (g/l)	60	36 (25–47)
α_1-agp (g/l)	69	1.35 (0.57–4.18)
Bilirubin (μmol/l)	73	6.0 (3.0–41)
ALP (μkat/l)	72	4.85 (2.2–65)
ASAT (μkat/l)	73	0.51 (0.23–18.5)
ALAT (μkat/l)	73	0.4 (0.09–10.6)
Categorical covariate		
Sex	31 female patients (52 profiles) 14 male patients (23 profiles)	

BSA, body surface area; $CL_{Cr,}$ creatinine clearance; α_1-agp, alpha$_1$-acid glycoprotein; ALP, alkaline phosphatase; ASAT, aspartate aminotransferase; ALAT, alanine aminotransferase.

quantification (LOQ) using 500 μl plasma sample solution was tested at 0.017 μM ($n = 10$, coefficient of variation (CV) = 13.4% accuracy (measured/nominal) 99.7%). For inter-assay precision, quality controls with 0.0843, 5.057 and 13.49 μmol/l of paclitaxel were used resulting in CVs of 7.3, 6.3 and 2.2% and accuracies of 99.1, 98.5 and 100.5%, respectively.

The analytical procedure for CrEL was based on a colorimetric dye-binding assay using Coomassie Brilliant Blue G-250 [14, 15]. The LOQ of this procedure was 0.50 μl/ml, with an accuracy >93.67% and within-run and between-run precision of <9.47% and <1.83%, respectively, in the tested concentration range (i.e. 0.50–10.0 μl/ml). Observations between the limit of detection and LOQ were also used in the analysis. For inter-assay precision, quality controls with 2, 4 and 8 μl/ml of CrEL were used resulting in CVs of 6.96, 3.88 and 11.3% and accuracies of 92.5, 92 and 90.1%, respectively.

Unbound concentrations were obtained from an equilibrium dialysis method as described earlier in Refs. [9,16] where 2 μl of a [^{3}H] paclitaxel solution in ethanol was added to 300 μl of plasma prior to incubation. Preliminary experiments established that (*i*) the time to reach equilibrium between plasma proteins and the buffer compartment for paclitaxel is attained at around 20 h, both in the presence and absence of CrEL; and (*ii*) CrEL did not cross the membrane, as indicated by the absence of detectable levels in the buffer compartment after dialysis [5]. The ratio of [^{3}H] measured in the buffer and plasma after dialysis was taken as an estimate of paclitaxel-free fraction (f_u). Because the volume shift during dialysis was negligible (<10%), the results were used directly without applying a correction factor. The addition of tritiated paclitaxel was done in all of the samples, including the 'blank' samples that were taken from the patients prior to drug administration. During the establishment of the method [16], duplicate or triplicate plasma samples with differing paclitaxel f_u values (spiked CrEL concentrations of 0, 0.10, 0.25, 1.0, 2.5 or 5.0 μl/ml) were subjected to repeated analysis on 6 consecutive days. The mean relative deviation of these samples was 9.2%, assuring high discriminatory power in the detection of changes in the paclitaxel f_u in the presence of CrEL. The within-run and between-run variability, expressed as a CV were <9.2% and <3.3%, respectively, at the 6 CrEL concentrations analysed and the LOQ of the free fraction ratio was 1%. Unbound concentrations were obtained by multiplying the measured total concentration with the estimated f_u.

2.2. Pharmacokinetic analysis

The pharmacokinetic analysis was performed in two parts: (1) Validation of a previously developed mechanism-based pharmacokinetic model [9], including previously determined parameter values, referred to as Model A, by: (i) predictions of unbound paclitaxel based on Model A and dose, (ii) predictions of unbound paclitaxel from Empirical Bayes (EB) parameter estimates based on Model A, dose and observed unbound concentrations of paclitaxel, (iii) predictions of unbound paclitaxel from EB estimates based on Model A, dose, observed total concentrations of paclitaxel and CrEL and (iv) an investigation of whether the present data-set requires all of the structural model components of the previously developed model and whether any additional model components are necessary to achieve an adequate fit to the data. (2) Whether any parameter-covariate relationships can be identified based on the present data-set.

The previously developed mechanism-based model [9] described three types of data simultaneously; unbound and total plasma concentrations and blood concentrations of paclitaxel. The unbound concentrations were described with a linear three-compartment model. The total concentration (C_p) was described with the following equation:

$$C_p = C_u + B_{lin} * C_u + B_{CrEL} * C_u + B_{max} * C_u/(K_m + C_u) \quad (1)$$

where B_{lin} is the linear binding to the plasma components, B_{CrEL} is binding directly proportional to the observed concentrations of CrEL, [CrEL]; B_{max} is the maximal non-linear binding to the plasma components and K_m the concentration at half-maximal binding.

The previously developed model was challenged in a number of alternative models. Two and three compartment models with linear and/or Michaelis–Menten kinetics in elimination and distribution were tried.

Different combinations of linear and/or non-linear binding to plasma components and binding directly proportional to observed concentrations of CrEL were tried. The modelling of the binding components was performed as a simultaneous fit of unbound and total concentrations.

The model parameters were estimated in a non-linear mixed effects ('population') analysis, where data from all of the patients are analysed simultaneously. This requires models for interindividual and interoccasion variability in parameters. For both types of variability, log-normal parameter distributions were assumed and interoccasion (or course-to-course) variability was implemented as previously described in Ref. [17]. Residual error was modelled with an additive (ϵ_1) and a proportional part (ϵ_2), either of which was excluded if not necessary to adequately describe the data.

2.3. Covariate model building

An automated covariate model building within NONMEM [18] with an inclusion criterion of $P<0.01$ and an exclusion criterium $P<0.001$ was used. The covariates listed in Table 1 were tested on the following parameters: volume of distribution of the central compartment (V1), volume of distribution of the peripheral compartment (V2) and clearance (CL). Including highly correlated covariates such as body surface area (BSA), height and weight in a stepwise procedure is not recommended [19], so, initially, BSA was used as a size measure. Missing values were treated as the population median value. In addition, SEX, bilirubin, age, BSA, aspartate aminotransferase (ASAT), alanine aminotransferase (ALAT), alkaline phosphatase (ALP) and the plasma proteins, albumin and α_1-acid glycoprotein (α_1-agp), were tested as covariates on the binding parameters.

All analyses were performed with the first-order conditional estimation (FOCE) method with interaction in the NONMEM program, version V/VI beta [20]. The models can be implemented in NONMEM version V. NONMEM VI beta was used in order to shorten runtimes. Graphical diagnostics, using the Xpose program [21] and comparison of competing models using the objective function values (OFV) in the likelihood ratio test guided the model development. A difference in OFV of >10.83, corresponding to a significance level of $P<0.001$, was used for discrimination between two hierarchical models differing in one parameter.

FOCE with interaction was used since it has been shown to provide significance levels close to the nominal during covariate model building [22].

2.4. PK/PD modelling

The exposure–toxicity (PK/PD) relationship with ANC was modelled with the general, threshold, and AUC models. The basis for the general model is that the transformation of the plasma concentration most closely related to the toxicity is estimated as part of the model [11]. The result of this transformation can be thought of as a 'direct' effect, which is not observable, but ultimately leads to the observed effect. The model is not relying on such a direct effect to exist, but it is a useful hypothesis for describing the model. The direct effect, E_{dir} is a function of the drug concentration. The observed effect, E_{obs} is related to the area under the E_{dir}–time curve, $AUCE_{dir}$. Sigmoidal E_{max} models are used to describe the relationships as follows:

$$E_{dir} = E_{dir,max} * C^{\beta}/(EC_{50}{}^{\beta} + C^{\beta}) \quad (2)$$

$$E_{obs} = E_{obs,max} * AUCE_{dir}^{\gamma}/(AUCE_{dir,50}^{\gamma} + AUCE_{dir}^{\gamma}) \quad (3)$$

where β and γ are sigmoidicity factors. Since E_{dir} is not observed, $E_{dir,max}$ only scales $AUCE_{dir,50}$ and can be set to 1. The parameter $AUCE_{dir,50}$ is the duration of maximal direct effect needed to produce half the maximal observed effect. The observed effect was modelled as a relative effect:

$$ANC = BASE* (1 - E_{obs,max} * AUCE_{dir}^{\gamma})/(AUCE_{dir,50}^{\gamma} + AUCE_{dir}^{\gamma}) \quad (4)$$

where ANC is the observed nadir, BASE is the baseline and $E_{obs,max}$ has a maximal value of 1 indicating that if we give a high enough dose the blood cells will be wiped out entirely. The threshold and AUC models are special cases of the general model. For the threshold model, β is infinitely high and EC_{50} is equivalent to the threshold concentration and for the AUC model β is 1 and $EC_{50} \gg C$. For the threshold modelling, β was fixed at 100, EC_{50} (the threshold concentration), $AUCE_{dir,50}$, γ and BASE were estimated. When developing the AUC model, $AUCE_{dir}$ was set to the area under the plasma concentration-time curve and BASE, γ and $AUCE_{dir,50}$ were estimated.

In these models, C_p and C_u are used separately as predictors of toxicity. However, these are not nested models and no significance could be attributed to differences in the goodness of fits' (OFVs). In order to obtain this, both models were compared to a full model including the sum of C_p and C_u, where the latter was scaled with a fixed effects parameter estimated as part of the model.

Log-normal distribution was used when modelling interindividual variability. Residual error (which in this case includes interoccasion variability was modelled with an additive (ϵ_1) and a proportional part (ϵ_2), each of which can be excluded if not needed to describe the data. As in the pharmacokinetic analysis, the programs NONMEM and Xpose were used, but a less strict significance criterion ($P<0.01$) was used.

3. Results

3.1. Pharmacokinetics

Observed concentrations of CrEL, unbound (C_u) and total concentrations (C_p) of paclitaxel are shown in Fig. 1. The unbound concentrations were well described by the earlier model. As can be seen in Fig. 2, the predictions from model A and dose (i) (left panel) deviated to some extent from the line of identity. The bias in etas (interindividual variability + interoccasion variability), in the predictions from EB estimates based on Model A, dose and observed unbound concentrations (ii) (middle panel) calculated as % deviation from median 0, was −19% for CL, 14% for V1 and 10% for V2. The predictions from model A, dose and observed total paclitaxel concentrations and CrEL (iii) (right panel) were almost as good as in (ii).

When fitting the model to the new data, there was only support for two compartments i.e. adding a third compartment did not improve the fit. Therefore, a two-compartment linear model was used to describe the unbound concentration of paclitaxel. This model is referred to as the basic model in Table 2. No correlation between dose and individual CL and V could be seen and addition of non-linear components in distribution and/or elimination did not improve the fit.

Exclusion of BSA on CL, V1 and V2 and bilirubin on CL from the final model resulted in increases in OFV with values of 16.0, 66.1, 11.5 and 39.3, respectively. The parameter estimates with relative standard error (RSE) and equations for the typical values are given in Table 2.

Interindividual variability was estimated on CL and V2 and was rather low, 19 and 17%, respectively. Interoccasion variability did not significantly improve the fit of the final model. A proportional residual error model was used and was estimated to 17.8%.

Bound plasma concentration was modelled with the same components as in the previous model (see Eq. (1): (1) a binding component directly proportional to CrEL concentrations, (2) a linear binding and (3) a non-linear binding to other plasma components. Each of these components was significant as when each of the components (1)–(3) was omitted from the final model, the OFV increased with values of 208, 16.6 and 52.6, respectively. The requirement to include multiple

Table 2
Pharmacokinetic parameters with RSE (%) for unbound and total paclitaxel concentrations

Parameter	Basic model C_u	Final model[a] for C_u only	Final model[b] for C_u and C_p
CL[c] (l/h)	332 (5.7)	351 (3.3)	343 (3.5)
V1[d](l)	414 (18)	428 (8.2)	418 (7.1)
V2[e] (l)	969 (4.7)	1030 (5.5)	1010 (4.2)
Q (l/h)	194 (26)	183 (15)	188 (13)
B_{lin}			3.31 (28)
B_{CrEL}			4.46 (7.2)
B_{max}[f]			0.212 (34)
Slope (B_{max}/K_m)			9.41 (9.4)
IIV_{CL} (CV%)	26 (26)[g]	19 (27)[g]	20 (24)[g]
IIV_{V2} (CV%)	20 (55)[g]	17 (52)[g]	16 (37)[g]
IIV_{BCrEL} (CV%)			14 (31)[g]
BSA on V1		1.77 (15)	1.45 (14)
BSA on V2		0.844 (25)	0.868 (18)
BSA on CL		0.779 (18)	0.65 (22)
BIL on CL		−0.0146 (13)	−0.012 (21)
α_1-agp on B_{max}			1.09 (14)
$\epsilon_{2\ Cu}$ (%)	21.2 (7.6)	17.8 (9.2)	17.5 (8.9)
$\epsilon_{2\ Cp}$ (%)			14.9 (8.8)
OFV	−1602.987	−1707.234	−2202.778

RSE, relative standard error; BIL, bilirubin; CL, clearance; V1, volume of distribution of the central compartment; B_{max}, is the maximal non-linear binding to the plasma components; B_{lin}, is the linear binding to plasma components; OFV, objective function value; B_{CrEL}, is binding directly proportional to the observed concentrations of CrEL[CrEL]; V2, volume of distribution of the peripheral compartment; K_m, the concentration at half-maximal binding; Q, intercompartmental clearance; IIV, interindividual variability; ϵ_2, proportional residual error; α_1-agp, alpha$_1$-acid glycoprotein. CV% is coefficient of variation in%.

[a] Parameter estimates for the typical individual with BSA 1.76 BIL 6.0.

[b] Parameter estimates for the typical individual with BSA 1.76 BIL 6.0 α_1-agp 1.35.

[c] CL = 343 * (1 + 0.65*(BSA−1.76))*(1−0.012*(BIL−6)).

[d] V1 = 418*(1 + 1.45*(BSA−1.76)).

[e] V2 = 1010*(1 + 0.868*(BSA−1.76)).

[f] B_{max} = 0.212*(1 + 1.09*(α_1-agp-1.35)).

[g] %RSE is related to estimate of ω^2.

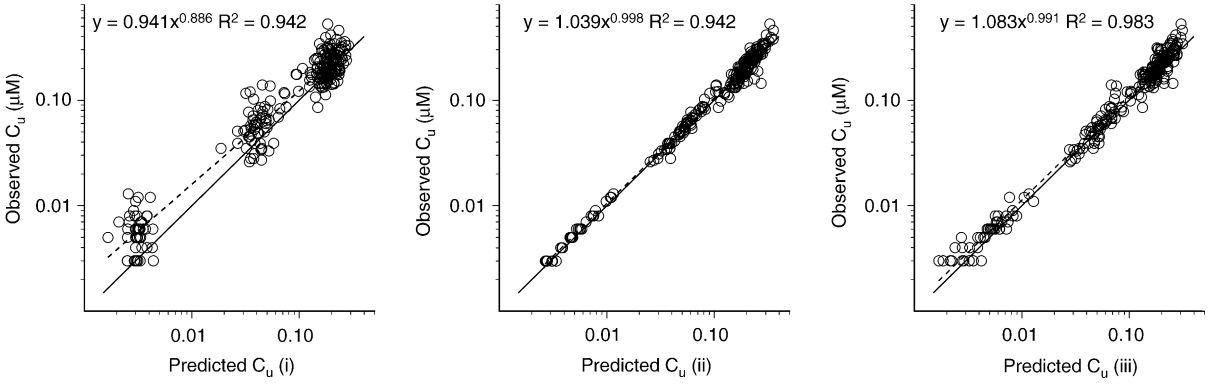

Fig. 2. Predictions based on: Model A and dose with no estimation (i), Empirical Bayes (EB) estimates based on Model A, dose and observed C_u (ii), EB estimates based on Model A, dose, C_p and [CrEL] (iii). Lines of identity (solid) and regression (dashed) are included.

plasma binding components is also evident from Fig. 3. The free fraction (f_u) of paclitaxel was higher at the early time points than at the later points, even though the concentration of CrEL was the same. This would imply that at higher concentrations the plasma protein binding is saturated. The non-linear binding parameters were estimated as maximal binding, B_{max}, and slope, (B_{max}/K_m), in order to avoid correlation problems between B_{max} and K_m when there are difficulties in accurately estimating both parameters. Parameter estimates and relative standard errors are given in Table 2. The estimated B_{max} was low compared with concentrations of the plasma proteins. This could be due to the difficulty of estimating the separate parameters when both linear and non-linear binding components are included.

Addition of interindividual variability in binding to CrEL resulted in a drop of 14.5 in OFV and was estimated to 14%. Additional interindividual variability in the binding parameters did not improve the fit. The variability in binding could include the variability in the CrEL assay since the observed values are treated as exact values.

Including α_1-agp as a covariate on B_{max} resulted in a drop in the OFV of 11.4. According to that relationship an increase in α_1-agp of 0.1 g/l will cause an increase in B_{max} with 0.023 μM. In this population, typical values ranged from 0.032 to 0.866 μM.

In the final model for C_u and C_p, a change in BSA of 0.1 m^2 caused changes in V1 and V2 of 60.6 and 87.7 l, respectively and a typical change in CL of 22.3 l/h. Typical values in the population ranged from 169 to 654 l for V1 and from 651 to 1352 l, for V2. An increase in bilirubin of 10 μM caused a typical change in CL of 41.1 l/h. The covariate relationships for CL are further illustrated in Fig. 4.

Population predictions (left panel) based on model, covariates (including CrEL concentrations for the prediction of total paclitaxel) and dose and individual predictions (right panel) from the empirical Bayes estimates based on model, covariates, CrEL concentrations and observed concentrations of unbound and total paclitaxel are shown in Fig. 5.

3.2. PK/PD modelling

Parameter estimates with relative standard errors for the AUC and threshold models are given in Table 3. The threshold model best described the ANC data both when unbound and total concentrations were used. The threshold concentrations were estimated as 0.00615 and 0.0615 μmol/l, respectively. The time above the threshold concentration required to cause a reduction in ANC of 50% was estimated as 8.81 and 7.5 h, respectively. In Fig. 6, the observed nadir versus predicted

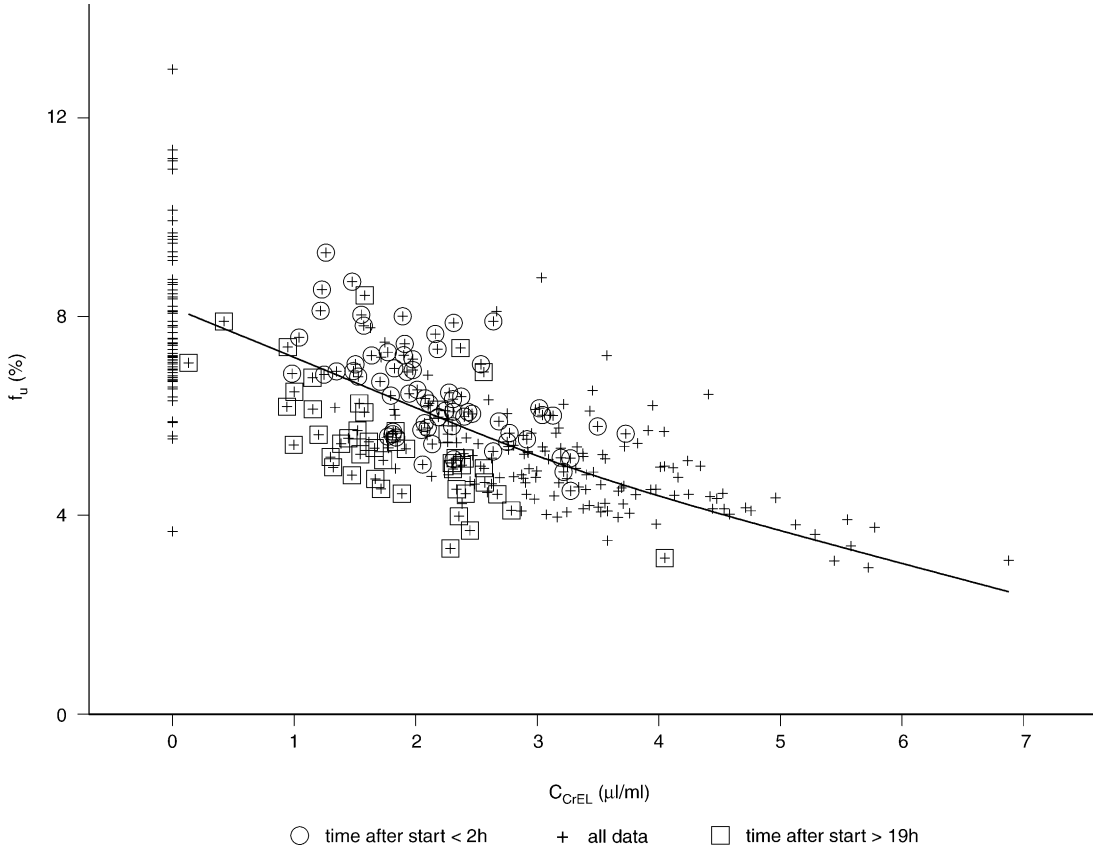

Fig. 3. Observed free fraction (f_u) of paclitaxel versus observed concentrations of CrEL. The line is a spline smooth for the individual predictions of f_u.

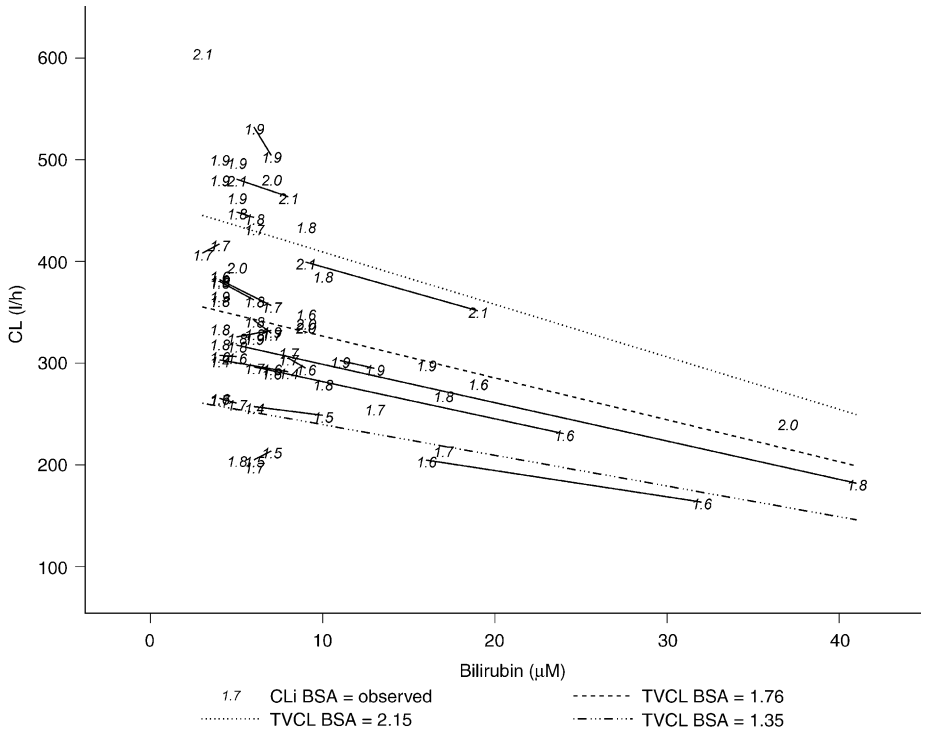

Fig. 4. Typical values of clearance in the population, TVCL, with maximum, median and minimum values of body surface area (BSA) (dotted lines) and individual predictions of clearance, CLi, (symbol showing the observed BSA value) versus bilirubin. Changes within an individual are illustrated by the solid lines.

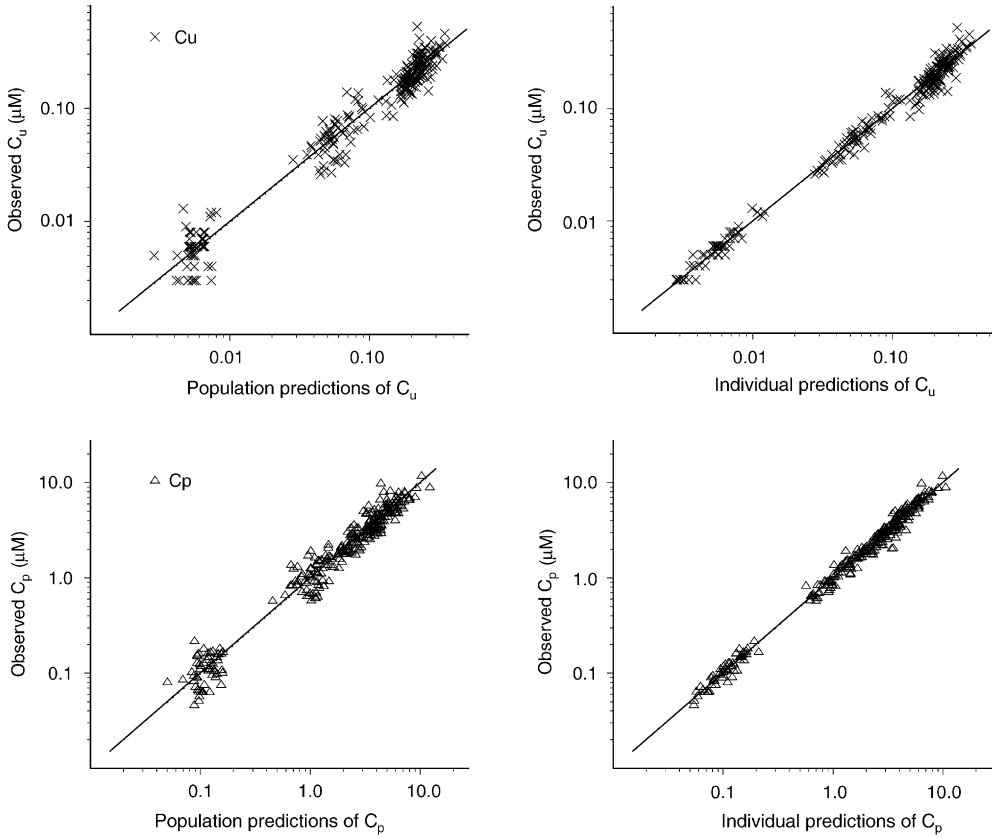

Fig. 5. Population predictions (left panel) based on the final model, covariates (including [CrEL] for prediction of total paclitaxel) and dose; individual predictions (right panel) from the EB estimates based on model, covariates, [CrEL] and observed concentrations of unbound and total paclitaxel.

Table 3
Pharmacodynamic parameter estimates with relative standard errors based on unbound and total plasma concentrations of paclitaxel

$C_{paclitaxel}$	C_u		C_p	
Model	AUC	Threshold	AUC	Threshold
OFV	180.8	171.1	184.4	173.5
BASE	5.67 (7.6)	5.57 (8.5)	5.64 (7.9)	5.52 (7)
EC_{50} (μmol/l)		0.00615 (3.2)		0.0615 (0.085)
$AUCE_{dir,50}$[a]	0.476 (13)	8.81 (20)	6.93 (14)	7.5 (16)
ϵ_1 ($\times 10^9$/l)	0.884 (23)	0.568 (105)	0.888 (29)	0.399 (56)
ϵ_2 (%)	15 (53)	24.6 (74.8)	16.9 (52)	29.9 (22)
IIV_{BASE} (CV%)	35 (31)[b]	38 (52)[b]	34 (32)[b]	41 (34)[b]

CV% is coefficient of variation in%; BASE, baseline; OFV, objective function value; EC_{50}, threshold concentration; $AUCE_{dir,50}$, duration of maximal direct effect needed to produce half the maximal observed effect; ϵ_1, additive residual error; ϵ_2, proportional residual error; IIV, interindividual variability.

[a] (h) for threshold model, (μmol*h/l) for AUC model.

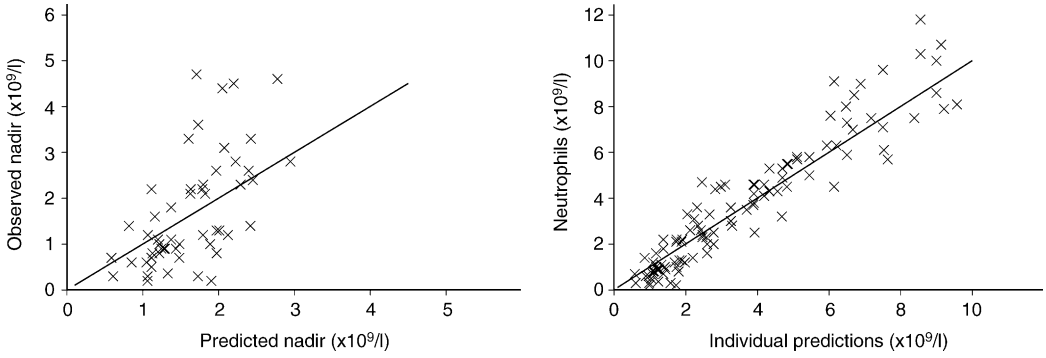

Fig. 6. Observed nadir versus predicted nadir based on the threshold model, unbound concentrations and baseline observations (left) and observed versus individual predictions of neutrophil counts from EB estimates based on the threshold model, unbound concentrations and observed neutrophils at baseline and nadir (right).

nadir from EB estimates based on the threshold model, unbound concentrations of paclitaxel and only baseline observations of neutrophils (left panel) and observed neutrophils versus individual predictions from EB estimates based on the threshold model, unbound concentrations of paclitaxel and baseline and nadir observations are shown. The general model (estimating beta) did not significantly improve the fits (ΔOFV was not greater than 2.1) and there were difficulties in obtaining successful estimation terminations. If successful, the relative standard errors were large (data not shown). Estimating E_{max} and the sigmoidicity factor, γ, did not improve the fit significantly, so these were both fixed at 1.

When the OFV of the threshold models for C_p and C_u were compared with the full model, including both C_p and C_u, a significant ($P = 0.0320$) improvement in the fit was noted when Cu was added as a predictor to the Cp model whereas in the opposite case, Cp added to the Cu model, no significant ($P = 0.1473$) improvement was observed.

4. Discussion

These data were well described by the previously developed model and also the unbound concentrations were well predicted from total plasma concentrations of paclitaxel, CrEL and the model. Both two and three compartment non-linear pharmacokinetic models have been used when describing paclitaxel pharmacokinetics [1,2,6]. In this study, there was not enough data to support more than two compartments. No dose dependence could be seen in the free concentrations. The typical value of CL in the population was somewhat lower than Model A (343 compared with 429 l/h). The volume of distribution at steady state was in good agreement (1428 compared with 1388 l). Thus, the present data supported the previously developed model, with the exception that a three-compartment model could not be identified. Furthermore, based on the previous model, total paclitaxel concentrations and CrEL concentrations, precise predictions of unbound paclitaxel concentrations could be made. This could be useful in at least two situations: (i) for historical data, where total paclitaxel concentrations and CrEL concentrations are available, unbound paclitaxel concentration can be predicted and used in developing PK/PD relationships, and (ii) as the CrEL assay is considerably simpler than the unbound paclitaxel assay, measuring only total paclitaxel and CrEL may be an alternative to measuring unbound paclitaxel.

BSA is widely used as a dosage measure in oncology, but its use has been questioned [23]. In this model, BSA, when introduced as a slope-intercept model, explained the variability in clearance and volume of distribution (V1 and V2). When a direct proportionality between BSA and parameters was tried, as dosing by BSA indicates, BSA explained the variability in clearance and volume of distribution of the central compartment, but the OFV was higher. However, for all three parameters, direct proportionality with BSA resulted in a better fit than not including BSA at all. In the final model, BSA was exchanged with weight or height. The OFV was lowest for BSA and highest for weight (data not shown), but since they are not nested models statistical significance by drop in OFV could not be stated.

Even if it is difficult to interpret the liver function (metabolic capacity of the liver) from markers like bilirubin, it can be an indicator of liver damage or obstruction of the biliary passages. Since paclitaxel is eliminated by metabolism and biliary excretion [24], it is reasonable to think that clearance would decrease with increasing bilirubin. It has also been reported that in patient groups with elevated transaminase and bilirubin levels the clearance of paclitaxel was decreased [25].

To validate the covariate model for unbound concentrations; we used the final C_u model to predict the unbound concentrations of the seven individuals from a previous study [9] based on dose and observed BSA and bilirubin. When plotted on a log-log scale (compare Fig. 2), the coefficient, power and r^2 were 1.31, 1.57 and 0.92, respectively.

Binding to CrEL explains most of the non-linear behaviour of paclitaxel in plasma and the binding component to CrEL was in good agreement with the parameter estimate in model A. In this study, we used total concentrations of CrEL, which is a simplification of the real situation since paclitaxel can only be trapped in the micelles. There could be several explanations as to why f_u is higher during the infusion, such as non-linear binding to a plasma component. In the absence of CrEL, paclitaxel is extensively bound in plasma where values of f_u between 5.4 and 13% have been reported [4,8,16]. In this study, the f_u in the pre-dose sample was on average (±standard deviation (S.D.)) 7.9±1.54% (range 3.7–13%, $n=69$). Binding of paclitaxel to the plasma proteins, albumin and α_1-agp, has been reported to be linear up to 6 μM [8]. As could be seen in Fig. 1, most of the total concentrations were higher than 6 μM except at the later time points. The population parameters of plasma binding showed some discrepancy compared with Model A that might be explained by difficulties in determine these parameters in relation to the extensive CrEL binding. Even though the estimated value of B_{max} is not near the concentration of α_1-agp in plasma, B_{max} increases with increasing α_1-agp, which would suggest that the capacity-limited binding is related to the binding to α_1-agp. However, since B_{max} is low it will be of minor importance in the total binding when CrEL is present, therefore, in this case, the effect of α_1-agp on B_{max} may have little or no clinical relevance.

The pharmacodynamic data did not contain enough information to be able to estimate all of the parameters of the general model adequately. The estimated threshold concentration based on the total concentration is in agreement with earlier reported values, but the time is shorter compared with previous studies, where 11.16 h above 0.1 μmol/l [10] and 17.4 h above 0.05 μmol/l [6] were predicted to yield a 50% decrease in ANC. The difference between the present and previous models can be explained by the difference in sigmoidicity factors. If the same threshold concentrations and gammas as reported earlier were used, time above the threshold in this study was estimated to 12.1 h above 0.1 μmol/l (γ 2.73) and 13.4 h above 0.05 μmol/l (γ 2.3). The PK/PD model based on unbound concentrations had a lower OFV, which would indicate that the toxicity is at least as well, or possibly better, explained by unbound, rather than total, concentrations. There was a significant difference when C_u was added as a predictor of toxicity to the C_p model, but the difference was relatively small. There was no real improvement in the 'goodness of fit' plots, so the advantage of using unbound instead of total concentrations needs to be confirmed in larger studies. The difference in OFV was less between the threshold and AUC model when unbound concentrations were used. In the previous study, we were not able to discriminate between the three models when unbound concentrations were used. This study included some more data, but since only the 3-h infusion schedule was used, the concentration–time profiles of unbound and total concentrations are rather similar which could be the reason that the threshold model best describes the data, regardless of which concentrations we used.

In conclusion, this study showed that with a sparse sampling in a larger population, it was possible to estimate the same mechanism-based model as the one developed based on frequent sampling. Although the previous model did not include covariates besides CrEL concentrations, it predicts well the unbound and total concentrations from this study, which would suggest that once the CrEL concentration is known, the unbound concentration can be predicted from total plasma concentrations and the model, without information about other patient demographics. For cases where the total paclitaxel and CrEL concentrations are not available, we have presented a model that can predict the unbound concentrations based on dose and covariates. The present analysis suggests that haematological toxicity may be better related to unbound than total paclitaxel concentrations, but also that further data are needed to establish an appropriate PK/PD model for unbound paclitaxel concentrations.

Acknowledgements

We are grateful to the patients who kindly participated in this study. We would also like to thank Britt Jansson, Eric Brouwer and Karin Sjöberg for their technical assistance, Siv Jönsson for many helpful discussions regarding model building and, finally, we thank the Swedish Cancer Society and Bristol Myers Squibb Clinical Oncology Research Department for their financial support.

References

1. Sonnichsen DS, Hurwitz CA, Pratt CB, Shuster JJ, Relling MV. Saturable pharmacokinetics and paclitaxel pharmacodynamics in children with solid tumors. *J Clin Oncol* 1994, **12**, 532–538.
2. Karlsson MO, Molnar V, Freijs A, Nygren P, Bergh J, Larsson R. Pharmacokinetic models for the saturable distribution of paclitaxel. *Drug Metab Dispos* 1999, **27**, 1220–1223.
3. van Zuylen L, Karlsson MO, *et al*. Pharmacokinetic modeling of paclitaxel encapsulation in Cremophor EL micelles. *Cancer Chemother Pharmacol* 2001, **47**, 309–318.
4. van Tellingen O, Huizing MT, Panday VR, Schellens JH, Nooijen WJ, Beijnen JH. Cremophor EL causes (pseudo-) non-linear pharmacokinetics of paclitaxel in patients. *Br J Cancer* 1999, **81**, 330–335.
5. Sparreboom A, van Zuylen L, Brouwer E, *et al*. Cremophor EL-mediated alteration of paclitaxel distribution in human blood: clinical pharmacokinetic implications. *Cancer Res* 1999, **59**, 1454–1457.
6. Gianni L, Kearns CM, Giani A, *et al*. Nonlinear pharmacokinetics and metabolism of paclitaxel and its pharmacokinetic/pharmacodynamic relationships in humans. *J Clin Oncol* 1995, **13**, 180–190.
7. Sykes E, Woodburn K, Decker D, Kessel D. Effects of Cremophor EL on distribution of Taxol to serum lipoproteins. *Br J Cancer* 1994, **70**, 401–404.
8. Kumar GN, Walle UK, Bhalla KN, Walle T. Binding of taxol to human plasma, albumin and alpha 1-acid glycoprotein. *Res Commun Chem Pathol Pharmacol* 1993, **80**, 337–344.
9. Henningsson A, Karlsson MO, Vigano L, Gianni L, Verweij J, Sparreboom A. Mechanism-based pharmacokinetic model for paclitaxel. *J Clin Oncol* 2001, **19**, 4065–4073.
10. Huizing MT, Keung AC, Rosing H, *et al*. Pharmacokinetics of paclitaxel and metabolites in a randomized comparative study in platinum-pretreated ovarian cancer patients. *J Clin Oncol* 1993, **11**, 2127–2135.
11. Karlsson MO, Molnar V, Bergh J, Freijs A, Larsson R. A general model for time-dissociated pharmacokinetic-pharmacodynamic relationship exemplified by paclitaxel myelosuppression. *Clin Pharmacol Ther* 1998, **63**, 11–25.
12. Minami H, Sasaki Y, Watanabe T, Ogawa M. Pharmacodynamic modeling of the entire time course of leukopenia after a 3-hour infusion of paclitaxel. *Jpn J Cancer Res* 2001, **92**, 231–238.
13. Beijnen JH, Huizing MT, ten Bokkel Huinink WW, *et al*. Bioanalysis, pharmacokinetics, and pharmacodynamics of the novel anticancer drug paclitaxel (Taxol). *Semin Oncol* 1994, **21**, 53–62.
14. Sparreboom A, Loos WJ, Verweij J, *et al*. Quantitation of Cremophor EL in human plasma samples using a colorimetric dye-binding microassay. *Anal Biochem* 1998, **255**, 171–175.
15. Brouwer E, Verweij J, Hauns B, *et al*. Linearized colorimetric assay for cremophor EL: application to pharmacokinetics after 1-hour paclitaxel infusions. *Anal Biochem* 1998, **261**, 198–202.
16. Brouwer E, Verweij J, De Bruijn P, *et al*. Measurement of fraction unbound paclitaxel in human plasma. *Drug Metab Dispos* 2000, **28**, 1141–1145.
17. Karlsson MO, Sheiner LB. The importance of modeling interoccasion variability in population pharmacokinetic analyses. *J Pharmacokinet Biopharm* 1993, **21**, 735–750.
18. Jonsson EN, Karlsson MO. Automated covariate model building within NONMEM. *Pharm Res* 1998, **15**, 1463–1468.
19. Derksen S, Keselman HJ. Backward, forward and stepwise automated subset selection algorithms: frequency of obtaining authentic and noise variables. *Br J Math and Stat Psych* 1992, **45**, 265–282.
20. Beal SL, Sheiner LB. *NONMEM Users Guides, NONMEM Project Group*. San Francisco, University of California at San Francisco, 1998.
21. Jonsson EN, Karlsson MO. Xpose—an S-PLUS based population pharmacokinetic/pharmacodynamic model building aid for NONMEM. *Comput Methods Programs Biomed* 1999, **58**, 51–64.
22. Wahlby U, Jonsson EN, Karlsson MO. Assessment of actual significance levels for covariate effects in NONMEM. *J Pharmacokinet Pharmacodyn* 2001, **28**, 231–252.
23. Ratain MJ. Body-surface area as a basis for dosing of anticancer agents: science, myth, or habit? *J Clin Oncol* 1998, **16**, 2297–2298.
24. Monsarrat B, Chatelut E, Royer I, *et al*. Modification of paclitaxel metabolism in a cancer patient by induction of cytochrome P450 3A4. *Drug Metab Dispos* 1998, **26**, 229–233.
25. Panday VR, Huizing MT, Willemse PH, *et al*. Hepatic metabolism of paclitaxel and its impact in patients with altered hepatic function. *Semin Oncol* 1997, **24** S11-34–S11-38.